Supplementary material

Electronic and optical properties of core-shell InAlN nanorods: a comparative study via LDA, LDA-1/2, mBJ, HSE06, G_0W_0 and BSE methods

Ronaldo Rodrigues Pela,[1] Ching-Lien Hsiao,[2] Lars Hultman,[2] Jens Birch,[2] and Gueorgui Kostov Gueorguiev[2]

[1)] *Supercomputing Department, Zuse Institute Berlin (ZIB), Takustraße 7, 14195 Berlin, Germany*[a)]

[2)] *Thin film Physics Division, Department of Physics, Chemistry and Biology (IFM), Linköping University, SE 581 83 Linköping, Sweden*

(Dated: 6 February 2024)

[a)] Electronic mail: ronaldo.rodrigues@zib.de

I. DOS OF INALN NRS

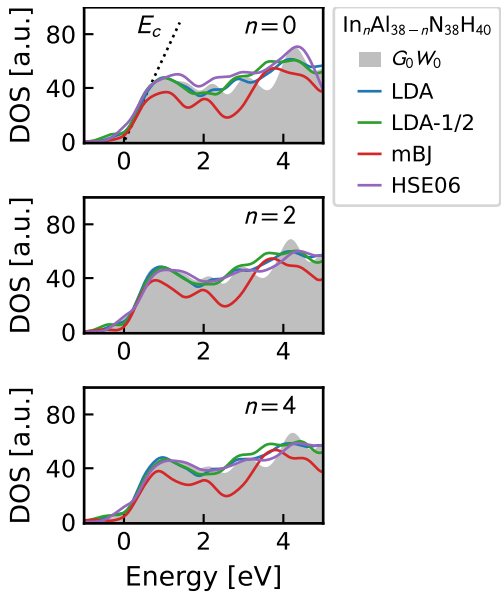

FIG. 1. DOS of passivated core-shell InAlN NRs for different In compositions. All energies are referred to E_c, the conduction band edge, when states are projected onto core atoms.

A. Peaks in DOS

TABLE I. Positions (in eV) of peaks P_1, P_2, P_3 and P_4 in DOS.

	$n=0$				$n=2$				$n=4$			
	P_1	P_2	P_3	P_4	P_1	P_2	P_3	P_4	P_1	P_2	P_3	P_4
G_0W_0	-5.00	-0.86	9.59	11.56	-5.22	-1.02	9.37	11.41	-5.44	-1.24	9.25	11.26
LDA	-4.95	-1.19	5.75	8.91	-4.96	-1.13	5.76	8.95	-4.94	-1.10	5.78	8.98
LDA-1/2	-3.78	-0.89	8.30	11.33	-3.84	-1.03	8.22	11.38	-3.99	-1.23	8.10	11.29
mBJ	-4.21	-0.94	7.65	10.48	-4.23	-0.96	7.57	10.48	-4.36	-1.14	7.48	10.38
HSE06	-5.21	-1.14	7.56	10.57	-5.16	-1.04	7.54	10.82	-5.25	-1.13	7.48	10.74

B. HSE06 and mBJ

HSE06 band gaps for AlN and InN are larger those of mBJ. On the other hand, for AlInN NRs, HSE06 predicts ΔE smaller than mBJ. Therefore, to confirm that DOS obtained with HSE06 for the NRs indeed precedes mBJ for conduction states, we performed a DOS calculation for AlN with VASP. The results are given in Fig. 2.

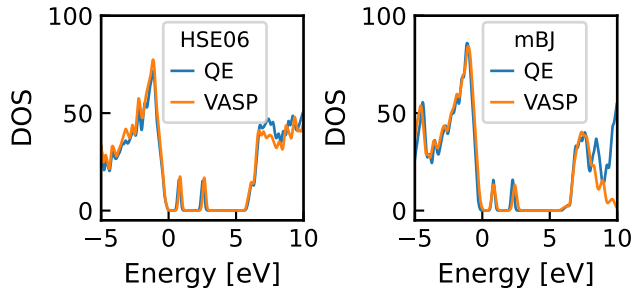

FIG. 2. Comparing the DOS of the AlN NR obtained with Quantum Espresso (QE) and VASP for the functionals: HSE06 (left) and mBJ (right).

II. OPTICAL PROPERTIES IN THE ENERGY RANGE OF 0-20 EV

A. AlN and InN

Figure 3 depicts the zz component of the dielectric function for energies between 0-20 eV.

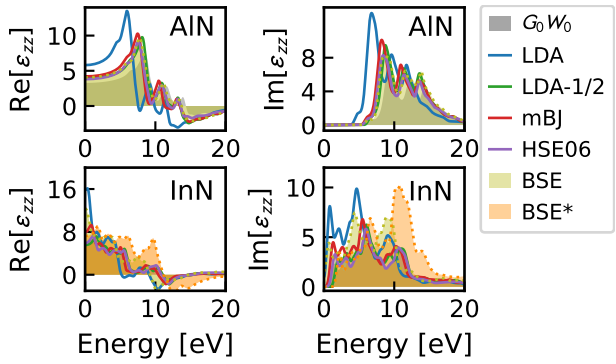

FIG. 3. zz component of the dielectric function: left, the real part, and right, the imaginary part.

B. Nanorods

Figure 3 depicts the *zz* component of the dielectric function in the energy range 0-20 eV.

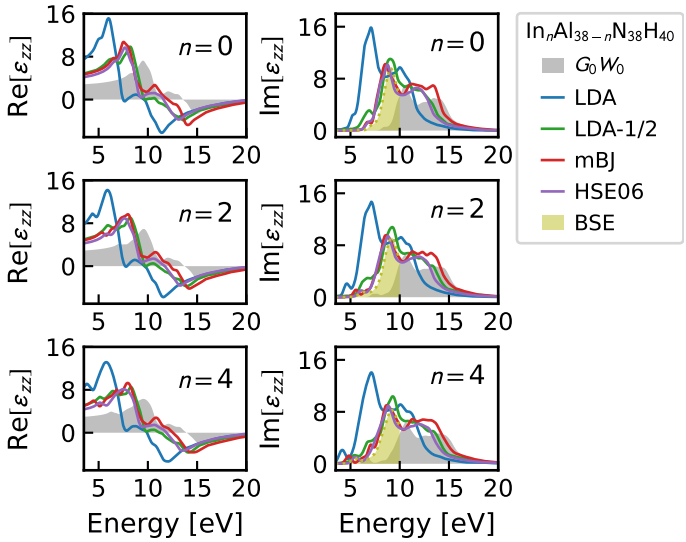

FIG. 4. *zz* component of the dielectric function: left, the real part, and right, the imaginary part. The label n denote the number of In atoms in the NR with chemical formula given by $In_nAl_{38-n}N_{38}H_{40}$.

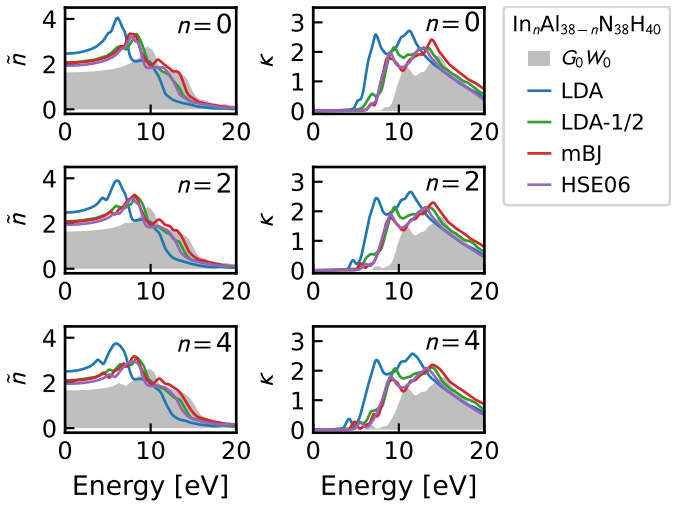

FIG. 5. Refraction index $\tilde{n}$ and extinction coefficient κ.

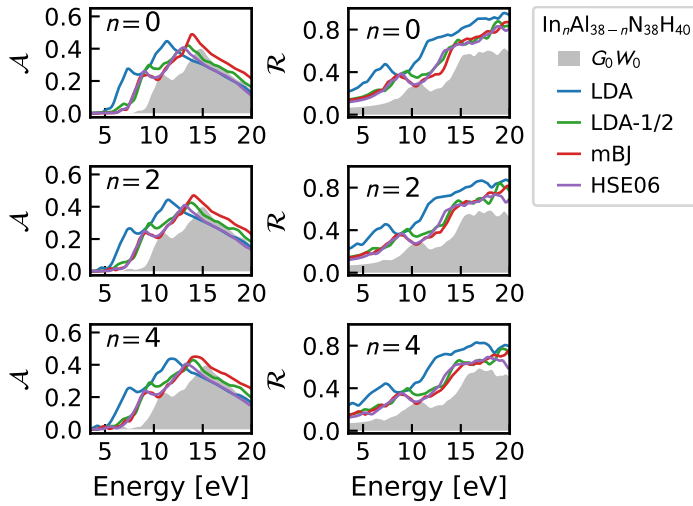

FIG. 6. Absorption $\mathscr{A}$ and reflectance $\mathscr{R}$.

III. CONVERGENCE BEHAVIOR

A. Bulk AlN and InN

Figures 7 and 8 show, for bulk AlN and InN, the convergence behavior of the G_0W_0 band gap. Two parameters are varied: the number of KS states (N_{bands}) and the planewave cutoff (E_{cut}) used to build the dielectric function. The convergence of G_0W_0 band gap is slower than that

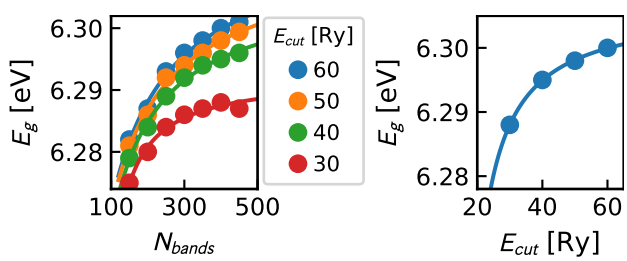

FIG. 7. AlN band gap obtained with G_0W_0: convergence behavior with respect to the number of bands (left) and the planewave cutoff for the dielectric function (right).

of DFT. Having a fully converged band gap is challenging, as employing a set of fully converged parameters comes with a very high computational cost. Therefore, we follow here an extrapolation procedure to evaluate the G_0W_0 band gap, adopting the expression[1–3]:

$$E_g(x) = E_g(\infty) + \frac{A}{x+B}, \tag{1}$$

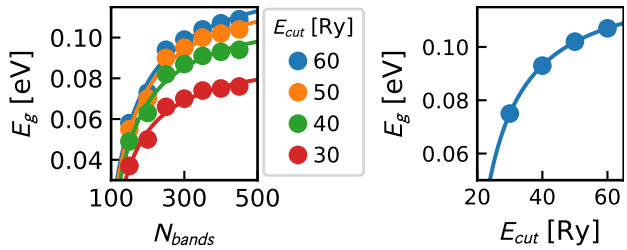

FIG. 8. Same as Fig. 7 for InN.

where $E_g(\infty)$, A and B are fit coefficients, and x is the convergence parameter being tested, which can be N_{bands} or E_{cut}. Assuming that the extrapolation with respect to E_{cut}, N_{bands} and the k-grid can be carried out separately, the extrapolated band gap E_g^{extr} can be evaluated as

$$E_g^{extr} = E_g^{ref} + \delta_{kpt} + \delta_{bands} + \delta_{cut}, \tag{2}$$

where $E_g^{ref} = E_g(N_{bands}^{ref}, E_{cut}^{ref}, k_{grid}^{ref})$ is the G_0W_0 band gap for a reference calculation employing N_{bands}^{ref}, E_{cut}^{ref}, and k_{grid}^{ref}. We adopt for AlN: $N_{bands}^{ref} = 200$, $E_{cut}^{ref} = 40$ Ry; and for InN: $N_{bands}^{ref} = 400$, $E_{cut}^{ref} = 50$ Ry; and, in both cases, k_{grid}^{ref} as $4 \times 4 \times 3$.

Then δ_{cut} and δ_{bands} are obtained as

$$\delta_{bands} = E_g(N_{bands} = \infty, E_{cut}^{ref}, k_{grid}^{ref}) - E_g^{ref}, \tag{3}$$

$$\delta_{cut} = E_g(N_{bands}^{ref}, E_{cut} = \infty, k_{grid}^{ref}) - E_g^{ref}, \tag{4}$$

and the contribution of the k-grid to the extrapolation is approximated as[1–3]:

$$\delta_{kpt} = E_g(N_{bands}^{ref}, E_{cut}^{ref}, k_{grid}^{large}) - E_g(N_{bands}^{ref}, E_{cut}^{ref}, k_{grid}^{ref}), \tag{5}$$

where $8 \times 8 \times 6$ is employed as k_{grid}^{large}.

Table II collects the relevant data regarding the extrapolation of the G_0W_0 band gap, and, for InN, G_0W_0@HSE06 as well.

B. Nanorods

1. Vacuum

In Eq. (9), Ω stands for the volume of the sample. However, in most of *ab initio* codes, including Quantum Espresso, Ω is treated as the unit cell volume. For systems with vacuum in

TABLE II. Contributions to the extrapolated G_0W_0 and G_0W_0@HSE06 band gaps. All quantities are given in eV.

	Starting point	E_g^{ref}	δ_{bands}	δ_{cut}	δ_{kpt}	E_g^{extr}
AlN	LDA	6.28	0.03	0.01	-0.03	6.29
InN	LDA	0.09	0.02	0.03	0.14	0.28
	HSE06	0.64	0.03	0.02	-0.04	0.65

the unit cell, such as the NRs studied here, the dielectric function must be corrected by a factor h equal to the ratio between the volumes of the cell and the sample. In terms of the geometry shown in Fig. 1, we have for the NRs

$$h = \frac{A_{cell}}{A_{nanorod}} = \frac{4L^2}{3d^2}, \tag{6}$$

where A_{cell} and $A_{nanorod}$ are the cross-sections of the unit cell and the NR, respectively.

Denoting ε'_{zz} as the dielectric function without the correction and ε_{zz}, the corrected one, then according to Eqs. (9) and (11), it follows that:

$$\mathrm{Im}[\varepsilon_{zz}] = h\mathrm{Im}[\varepsilon'_{zz}], \tag{7}$$

$$\mathrm{Re}[\varepsilon_{zz}] = 1 + h(\mathrm{Re}[\varepsilon'_{zz}] - 1). \tag{8}$$

Figure 9 depicts the convergence behavior of the dielectric function with respect to cell dimension L. These calculations refer to the AlN NR and have been carried out with LDA, and a similar

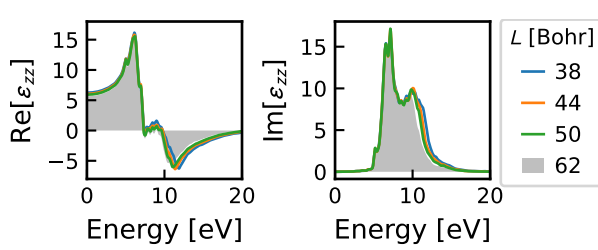

FIG. 9. Convergence behavior of the AlN NR - dielectric function obtained with LDA.

trend has been observed for the other cases. Fig. 9 shows that the size $L = 44$ Bohr, adopted for the NRs calculations reported in the present work, is sufficient to guarantee satisfactory convergence within the energy range of $0 - 20$ eV.

2. *Band gap*

Here, we discuss the precision level expected for our G_0W_0 calculations concerning the NRs. As for bulk AlN and InN, we check convergence with respect to N_{bands}, E_{cut} and the k-grid $1 \times 1 \times N_{kpt}$. For the sake of computational cost, we restrict the analysis to the ΓΓ band gap and the dielectric function of AlN.

Figure 10 depicts on the left side the impact of N_{kpt} and N_{bands} on the ΓΓ band gap. Since we adopted $N_{kpt} = 6$ and $N_{bands} = 900$, we estimate, by making the extrapolation procedure as described in III A, a correction of $\delta_{bands} = -0.06$ eV and $\delta_{kpt} = -0.08$ eV.

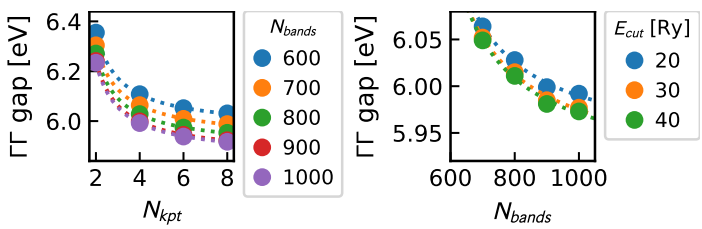

FIG. 10. Convergence behavior of ΓΓ band gap obtained with G_0W_0 for the AlN NR: impact of N_{bands} and N_{kpt} (left); and N_{bands} and E_{cut} (right).

On the right side of Fig. 10, the influence of N_{bands} and E_{cut} on the ΓΓ band gap is shown. Following the extrapolation procedure, we evaluate a correction of $\delta_{cut} = -0.03$ eV for the adopted $E_{cut} = 20$ Ry. Overall, by adding up δ_{bands}, δ_{kpt} and δ_{cut}, we expect that G_0W_0 band gaps are overestimated by about 0.2 eV.

Figure 11 presents the convergence behaviour of the imaginary part of dielectric function with respect to the vacuum layer (left), the number of bands (middle), and the number of k-points (right). Even though the G_0W_0 band gap requires more strict parameters for convergence, the dielectric function exhibits faster convergence.

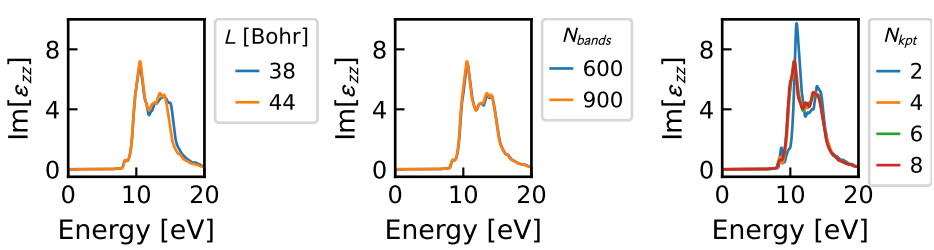

FIG. 11. Impact of the vacuum length, the number of bands, and the number of k-points on the dielectric function of AlN NR.

IV. QUANTUM CONFINEMENT AND BAND GAP

The expected band gap enlargement Δ due to quantum confinement effects can be estimated by considering a particle of mass μ confined inside a circular quantum well of radius r. Following Ref. 4, we have, in atomic units:

$$\Delta = \frac{a_{(0,0)}^2}{2\mu^* r^2}, \tag{9}$$

where $a_{(0,0)} = 2.40483$ is the first zero of $J_0(x)$, Bessel's function of order zero. To estimate Δ for the case of the NRs, we approximate μ by the reduced mass of the electron and the heavy hole, $\mu = (1/m_e + 1/m_{hh})^{-1}$. Taking the suggested values in Ref. 5: $m_e = \sqrt[3]{(m_e^{\perp})^2 m_e^{\parallel}} = 0.31$, in atomic units. m_{hh} is obtained from the Pikus-Bir parameters given in Ref. 5 as[6]

$$m_{hh} = -\sqrt[3]{(A_2 + A_4)^{-2}(A_1 + A_3)^{-1}}, \tag{10}$$

which gives $m_{hh} = 1.1$, in atomic units. Therefore $\mu = 0.24$.

Lastly, we consider a range for r between the radius of the inscribed and the circumscribed circles in the NRs. Taking into account the NR diameter of 14 Å, this implies that r lies between 6.06 and 7 Å. Applying Eq. (9) gives the range of 1.9-2.5 eV for Δ.

V. SHIFT IN THE DIELECTRIC FUNCTION

Figure 12 shows, for the NRs, $\mathrm{Im}[\varepsilon_{zz}]$ of the different DFT approaches blue-shifted by δ to better match BSE. In the case of G_0W_0, the dielectric function has been red-shifted. To plot these curves, we shift the vertical transitions in Eq. (9), so that the shifted dielectric function ε'_{zz} at a given frequency ω relates to the original ε_{zz} by:

$$\mathrm{Im}[\varepsilon'_{zz}(\omega)] = \mathrm{Im}[\varepsilon_{zz}(\omega - \delta)]\frac{(\omega - \delta)^2}{\omega^2}. \tag{11}$$

It is observed that, setting δ to 2.1, 0.1, 0.6 and 0.4 eV for LDA, LDA-1/2, mBJ and HSE06, respectively, leads to an very good agreement with $\mathrm{Im}[\varepsilon_{zz}]$ obtained with BSE. G_0W_0, on the other hand, can be fitted to BSE with a red shift of 1.4 eV

REFERENCES

[1] J. Klimeš, M. Kaltak, and G. Kresse, "Predictive GW calculations using plane waves and pseudopotentials," Physical Review B **90**, 075125 (2014).

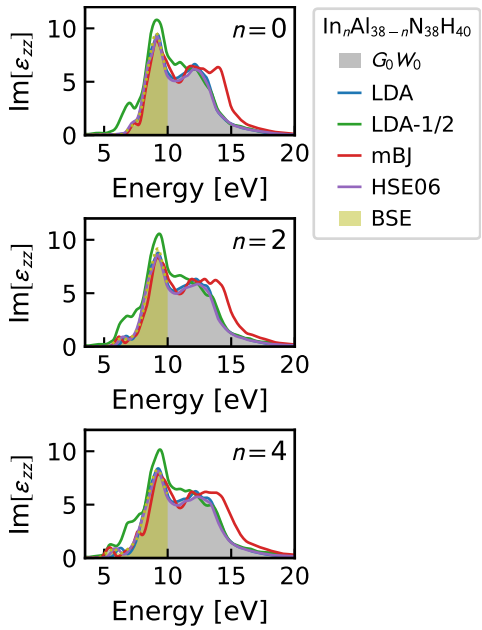

FIG. 12. $In_nAl_{38-n}N_{38}H_{40}$ core-shell NRs: Imaginary part of the dielectric function blue-shifted by δ. LDA, LDA-1/2, mBJ and HSE06 have been shifted by 2.1, 0.1, 0.6 and 0.4 eV, respectively. G_0W_0 has been red-shifted by 1.4 eV.

[2]D. Nabok, A. Gulans, and C. Draxl, "Accurate all-electron G_0W_0 quasiparticle energies employing the full-potential augmented planewave method," Physical Review B **94**, 035118 (2016), 1605.07351.

[3]R. R. Pela, U. Werner, D. Nabok, and C. Draxl, "Probing the LDA-1/2 method as a starting point for G0W0 calculations," Physical Review B **94**, 235141 (2016).

[4]R. W. Robinett, "Visualizing the solutions for the circular infinite well in quantum and classical mechanics," American Journal of Physics **64**, 440–446 (1996).

[5]I. Vurgaftman and J. R. Meyer, "Band parameters for nitrogen-containing semiconductors," Journal of Applied Physics **94**, 3675–3696 (2003).

[6]S. L. Chuang and C. S. Chang, "k.p method for strained wurtzite semiconductors," Physical Review B **54**, 2491–2504 (1996).